Uniform trapped fields produced by stacks of HTS coated conductor tape

2016 Supercond. Sci. Technol. 29 085008

(http://iopscience.iop.org/0953-2048/29/8/085008)

OPEN ACCESS
IOP Publishing
Superconductor Science and Technology
Supercond. Sci. Technol. **29** (2016) 085008 (10pp)
doi:10.1088/0953-2048/29/8/085008

Uniform trapped fields produced by stacks of HTS coated conductor tape

T B Mitchell-Williams[1], A Baskys[1], S C Hopkins[1], V Kalitka[2], A Molodyk[2], B A Glowacki[1,3,4] and A Patel[1]

[1] Department of Materials Science and Metallurgy, University of Cambridge, 27 Charles Babbage Road, Cambridge, CB3 0FS, UK
[2] ZAO SuperOx, 20-2 Nauchny Proezd, Moscow, Russia
[3] The Bernal Institute, Department of Physics and Energy, University of Limerick, Plassey, Ireland
[4] Institute of Power Engineering, ul. Mory 8, 01-330 Warsaw, Poland

E-mail: tbm23@cam.ac.uk

Received 15 April 2016, revised 24 May 2016
Accepted for publication 27 May 2016
Published 16 June 2016

Abstract

The trapped magnetic field profile of stacks of $GdBa_2Cu_3O_{7-x}$ superconducting tape was investigated. Angled stacks of superconducting tape were magnetized and found to produce very uniform trapped field profiles. The angled stacks were made of 12 mm × 24 mm solder coated tape pieces and were bonded together following a brief consolidation heat treatment. Layering multiple stacks together and adding a ferromagnetic plate beneath the samples were both found to enhance the magnitude and uniformity of the trapped field profiles. Stationary and time-dependent critical state finite element models were also developed to complement the experimental results and investigate the magnetization process. The size and shapes possible with the angled stacks make them attractive for applications requiring uniform magnetic fields over larger areas than can be achieved with existing bulk rings or tape annuli.

Keywords: HTS tape, stacks of tape, composite bulk superconductor, numerical modelling, trapped field magnets, magnetic measurements, uniform magnetic fields

(Some figures may appear in colour only in the online journal)

1. Introduction

Stacks of superconducting tape have been demonstrated to act as efficient trapped field magnets with fields of more than 7.9 T trapped in a 10 mm × 10 mm sample [1]. Furthermore, their thermal stability at low temperatures gives them advantages over bulk superconductors when pulse magnetized [2].

Uniform magnetic fields are required for portable, small-scale NMR/MRI devices. Superconducting trapped field magnets in the form of ring shaped bulks [3, 4] and stacks of tape annuli [5, 6] that act as persistent mode coils have been developed. In all these cases, the central region of the field source object is not carrying net current. This is conceptually similar to permanent magnets which produce a field equivalent to that produced by surface currents alone. The size of the uniform field region available through these approaches are currently limited by the growth of bulk superconductors and the width of coated conductor tape respectively. Stacked tape arrays with crossed tape pieces have been shown to generate more uniform trapped field profiles over a larger area than single bulks and conventional tape stacks [7, 8]. However, in these structures the top layers of tape have a greater influence on the trapped field measured above the stack, which limits uniformity. Previous work using Roebel cable offcuts demonstrated that an angled stack arrangement of tapes could produce even more uniform trapped field profiles than simple 'criss-crossed' arrays of tape [9].

Self-supporting stacks can be produced from solder coated tape [10]. The current work reports highly uniform trapped field profiles produced by self-supporting angled

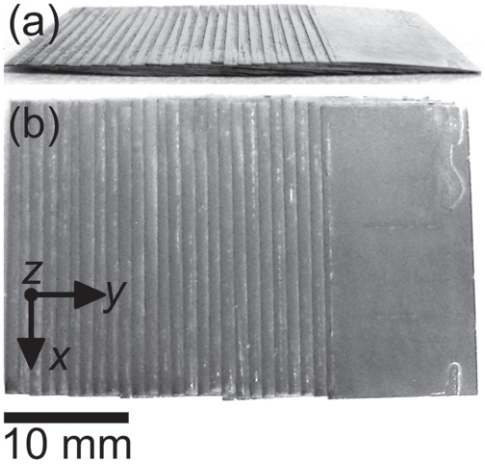

Figure 1. (a) Profile and (b) plan view of a single angled stack, stack A. The stack was constructed of 26 tape pieces each 12 mm × 24 mm in size, offset 1 mm laterally to adjacent pieces and at angle of 5.4° to the horizontal. The stack thickness was 1.2 mm.

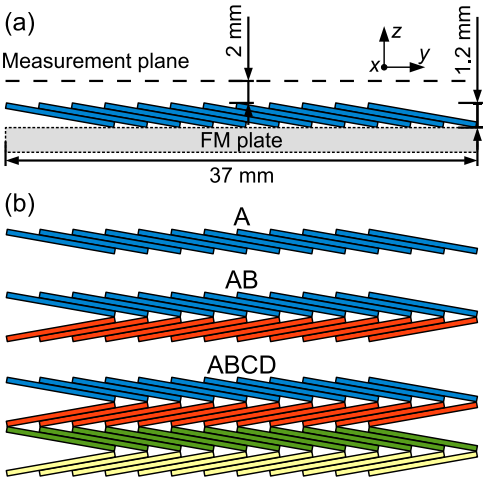

Figure 2. (a) Schematic showing measurement plane, axes and position of ferromagnetic (FM) plate, when used. (b) Schematic showing the different layers of stacks tested in the current work. The individual stacks A, B, C and D were all equivalent. Not to scale, individual stacks contained 26 tape pieces.

stacks of tape made from 12 mm wide solder coated tape. Additionally, layering of the stacks and the presence of a ferromagnetic (FM) plate beneath the sample have been demonstrated to increase the trapped field magnitude.

2. Stack geometry, fabrication and measurement method

2.1. HTS tape properties

Solder coated superconducting tape provided by SuperOx [11] was used in the current work to produce self-supporting angled stacks. The tape was 12 mm wide, 94 μm thick and had a minimum self-field I_c of 400 A at 77 K. The substrate was 60 μm thick non-magnetic Hastelloy® C276, the buffer and $GdBa_2Cu_3O_{7-x}$ (REBCO) layers followed the conventional IBAD-PLD architecture with a ~1.5 μm thick HTS layer. The tape had a 1 μm thick silver layer, 5 μm thick copper layer and 10 μm thick lead–tin eutectic solder layer on either side of the tape.

2.2. Stack geometry and fabrication

Following from previous work [9], an angled stack arrangement of tapes was investigated. The superconducting tape was cut into 24 mm long pieces. To form a single angled stack, 26 of these were arranged so the relative offset between pieces was 1 mm in the tape width direction (y-axis in figures 1 and 2). There was no offset in the tape length direction (x-axis in figures 1 and 2). All tape pieces were oriented in the same way with the HTS layer closer to the top surface ($+z$ side) than the Hastelloy® substrate. The tapes were held in place by a custom-made aluminium rig during assembly. The tape stacks were heated to 210 °C for 5 min to solder them together. Following this procedure, four self-supporting stacks were produced of the same geometry and specification; A, B, C and D.

In addition to single stacks several layers of the stacks were investigated as shown schematically in figure 2(b). These samples were referred to as A, AB and ABCD. Furthermore, it has been shown by Philippe *et al* [12] that a plate of soft FM material beneath a bulk REBCO superconductor can enhance the trapped field measured above it, so samples with a soft FM plate beneath were also characterized. The position of this plate relative to the stack, when used, is shown in figure 2(a). The plate was 0.85 mm thick mild steel cut to the same area as the stacks, 37 mm × 24 mm.

2.3. Scanning Hall probe magnetometry

The samples were field cooled (FC) to 77 K in liquid nitrogen in an applied field of 0.20 T. The field was applied using an electromagnetic coil and was ramped down to zero at a rate of 6.7 mT s^{-1} once the sample had reached 77 K. The trapped magnetic field profile was characterized by scanning a Hall probe (Arepoc HHP-VA) 2 mm above the sample surface. The bespoke mechanical stage was controlled by software developed in-house. The probe control current was nominally 10 mA and the sensitivity was 0.0522 V T^{-1}. The lateral step size was 0.25 mm for trapped field profile measurements in the y direction. For full area field maps, the step size was 0.5 mm in the x and y directions. Scans were started 300 s after magnetization to avoid significant effects from flux creep.

Flux creep measurements were also performed using the Hall probe system. The trapped magnetic field at a height of 2 mm above the centre of the sample was measured for ~4 h at 10 s intervals following magnetization.

2.4. Magnetic properties of the FM plate

The magnetic properties of the FM plate were measured using a sensitive vibrating sample magnetometer (PMC MicroMag 3900 Series VSM). A small sample, approximately

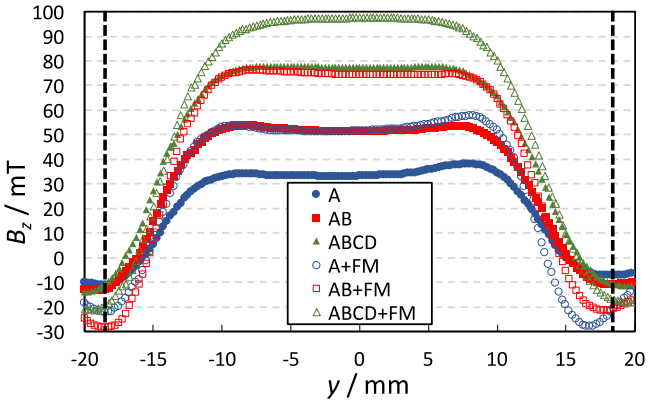

Figure 3. Trapped field profiles of the layered stacks with and without the ferromagnetic plate (FM). The stacks were field cooled to 77 K. The measurement height was 2 mm. Vertical dashed lines indicate sample dimensions.

$0.85\,\text{mm} \times 0.66\,\text{mm}^2$, was prepared from the same material as the FM mild steel plate. The sample was magnetically soft and displayed virtually no remanence. The relative permeability, μ_r, calculated from the initial gradient of the magnetization curve was ~10.

3. Trapped field profile results

3.1. Angled stacks of tape

The trapped field profiles shown in figure 3 have good uniformity. Having several layers of the stacks, as in samples AB and ABCD, led to a smoother trapped field profile than the single stack alone. Also, the asymmetry present in the trapped field profile for the single stack A was supressed when it was layered with additional stacks. The asymmetry in the field profile for a single stack is expected due to the nature of the stacking configuration and the property being measured; the z component of the magnetic field. As will be discussed in section 4.5 and appendix B, the angled stack can be thought of as similar to a coil with the edge segments contributing a net current.

To quantify and compare the uniformity of the field profiles, a roughness metric, R_{rms}, analogous to surface roughness, was used in a similar way to previous work [9]. This was a measure of the average variation away from the mean trapped field and is defined in appendix A. The data from the central 10 mm of the field profiles were used to calculate the mean trapped field, B^* and the profile roughness, R_{rms}. The values for each of the samples are summarized in table 1.

Layering stacks together increased the trapped field as did the addition of the FM plate beneath the samples. The magnitude of the increase resulting from doubling the number of stacks was approximately the same as that from the addition of the FM plate beneath the sample. The field enhancement due to the presence of the FM plate can be explained by considering the magnetic circuit around the sample when magnetized. The FM plate has a higher relative magnetic permeability, μ_r, than liquid nitrogen and so reduces the reluctance of the circuit surrounding the sample, reducing the stray field and enhancing the field magnitude above the sample surface.

Table 1. Trapped field profile roughness data.

Sample	Mean trapped field[a], B^* (mT)	Profile roughness[b], R_{rms} (mT)	Ratio, R_{rms}/B^* (%)
A	33.6	0.67	2.0
AB	51.8	0.31	0.6
ABCD	77.6	0.13	0.2
A + FM	51.7	0.77	1.5
AB + FM	74.6	0.38	0.5
ABCD + FM	97.3	0.38	0.4

[a] Mean trapped field for the central 10 mm of the sample.
[b] Details of how roughness was calculated are in appendix A.

Figure 4 shows the full area trapped field maps for several of the samples. It can be seen that the uniformity in the x direction (parallel to the length of the tape pieces) is good, as expected. The trapped field maps show that layers of the angled stacks can be magnetized to produce uniform trapped fields over large areas, with uniformity good in both directions. Furthermore, the FM plate does not distort the shape of the trapped field above the sample.

The angled stacks show several advantages over alternative methods for producing uniform fields using trapped field magnets such as tape annuli, bulk rings, tape coils or unsaturated bulks or stacks. Unlike annuli made out of either bulk rings [3] or stacks of tape [5], the size of the angled stacks is scalable and limited only by the method used for magnetization and amount of coated conductor available. Furthermore, the technical difficulties encountered with producing long lengths of coated conductor that can be used to produce a persistent mode coil are avoided because only relatively short sections of tape are required and no superconducting joints need to be created. Also, the uniformity, magnitude and reproducibility of the field profile is much better for angled stacks than an unsaturated bulk or conventional tape stack.

3.2. Magnetic flux creep measurements

The flux creep results for the single stack A are shown in figure 5. It can be seen that the decay follows the expected logarithmic dependence given by (1). The decay constant, a, was found to be less than 5% per time decade, which is comparable to bulks [13] and conventional stacks of tape [14, 15] at 77 K. The full area field profile remained unchanged in shape when measured after the flux creep experiment, the only perceptible change was the drop in magnitude predicted by logarithmic decay

$$\frac{\Phi(t)}{\Phi_0} = 1 - a \log\left(\frac{t}{t_0}\right) = 1 + a \log t_0 - a \log t. \quad (1)$$

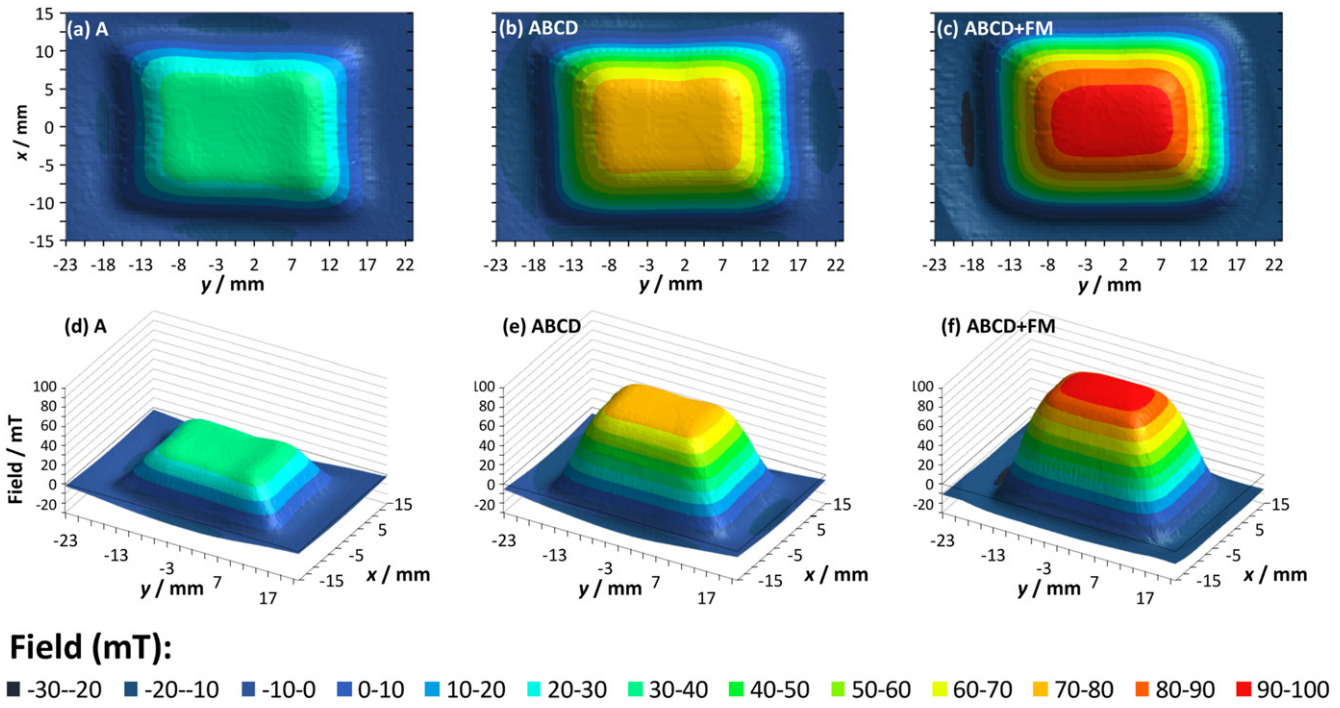

Figure 4. (a)–(c) Contour and (d)–(f) surface plots showing the trapped field profile for a single stack A, four layer stack ABCD and four layer stack with ferromagnetic plate beneath ABCD+FM. Measured at 77 K, 2 mm above the top surface.

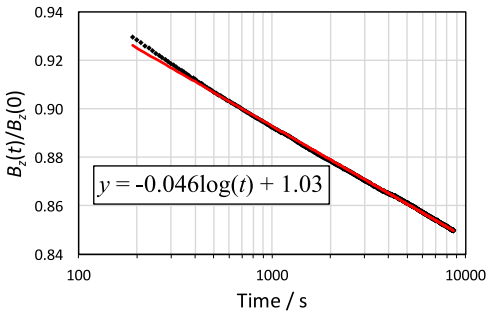

Figure 5. Flux creep for stack A. The rate of decay of flux, calculated from the gradient of the red trendline, is less than 5% per time decade.

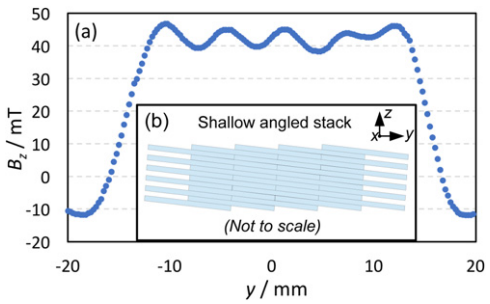

Figure 6. (a) Trapped field profile for the shallow angled stack. Inset, (b) shows the schematic structure of the stack. The stack was comprised of 30 pieces of tape each offset by 6 mm in the *y* direction with respect to adjacent pieces. The tape pieces were at an angle of 0.9° to the horizontal.

3.3. Alternative shallow angled stack

It was found that the angled stack behaves in a similar way to a coil, where the primary contribution to the trapped field magnitude was from the current near the edges of the sample. The currents induced in the tape pieces comprising the middle section of the angled stacks largely cancel each other out. This is discussed further in appendix B. Alternative designs for maximizing the trapped field magnitude whilst still retaining the field uniformity were considered. A shallower angled stack arrangement would give a larger engineering critical current density, $J_{c,eng}$, at the edges of the sample and therefore was predicted to give a higher trapped field magnitude.

An alternative angled stack with a shallower angle of tape pieces was designed, which had a similar cross-sectional area in the *y*–*z* plane to the angled stack A. The new stack was constructed and the field profile measured in the same way as the original angled stacks. Figure 6(a) shows the trapped field profile and 6(b) the stacking schematic for the shallow angled stack. It can be seen that although the average trapped field magnitude, B^*, was higher the uniformity was significantly poorer with a R_{rms} of 2.3 mT, corresponding to a relative ratio of >5.4%. The reason for this is likely due to the shallow angled stack being much more sensitive to small offsets and non-uniformities between tape pieces. In the stacking arrangement, the persistent current circulating in each piece of tape in the central region of the sample effectively cancels with the currents from adjacent pieces as discussed in appendix B. In the shallow angled stack, each piece of tape in the central region needs to exactly cancel out the contribution from its neighbours and hence a small offset or discrepancy in I_c between tape pieces can lead to larger scale non-uniformities in the trapped field profile. The more robust stacking

geometry of the angled stacks A, B, C and D accommodated for small discrepancies and misalignments more successfully. Therefore, the shallow angled stack remains an ideal case that requires more careful assembly to exploit its potential to achieve higher magnitude uniform fields.

4. Modelling trapped field profiles

4.1. Stationary study framework

Simple time-independent FEM modelling was conducted in COMSOL Multiphysics 5 using the AC/DC module and a stationary study. The approximation of uniform surface currents was used to simulate the superconducting surfaces on domains of the same cross-sectional dimensions as the real tape pieces. The models were 2D, only considering changes in the y–z plane shown in figure 2, assuming no variation in the x direction. This was a good approximation for investigating the trapped field profile in the y direction. More extensive time-dependent critical state modelling in sections 4.2 and 4.6, was performed for the single angled stack A, however, these models were only constructed for a single sample because they took a long time to solve and were often unstable due to the relatively high number of mesh elements and complex geometry.

4.2. Critical state modelling framework

The H-formulation for magnetic fields was used in COMSOL Multiphysics 5.0. The framework used an E–J power law to simulate the critical state, where E_x and J_x are the electric field and current density respectively. A field dependant n-value was used as in [16] based on data in [17] giving typical n-values of around 27 for our model

$$E_x = E_0 \left(\frac{J_x}{J_c(\underline{B})} \right)^{\left(\frac{n_0}{1+B/B_{0n}} \right)}. \quad (2)$$

The model used field cooling with a 0.1 T applied field which was enough to saturate the sample, with the field ramp rate being the same as for the experiment. Flux creep was modelled for a further 300 s after magnetization to match the time delay used for the experimental Hall scans. The field dependent n-value is most appropriate for the flux creep period as creep rates are sensitive to n-values. The Kim model was used to describe the dependence of the critical current density (equivalent to the engineering critical current density, $J_{c,eng}$, for the experiment) on field at 77 K

$$J_c(\underline{B}) = J_{c,eng} = \frac{I_{c0}}{wd\left[1 + \frac{\sqrt{k^2 |B_\parallel|^2 + |B_\perp|^2}}{B_0}\right]}. \quad (3)$$

It includes the J_c anisotropy of the tape integrated into the Kim law as used previously in [18], where the parameter k varies between 0 and 1. A full description of the parameters used is given in table 2. The motivation behind equation (3) is to use a simple mathematical framework that can easily fit typical measured $J_{c,eng}$ values for commercial superconducting tape for fields of up to 4 T, which certainly covers the field range in question at 77 K. The B_0 Kim law parameter was determined by fitting to data for typical SuperOx tape at 77 K. The anisotropy variation described by equation (3) does not give such a close fit to the available data as it describes smooth variation in J_c with angle rather than the sharper peak for real tape when the field is parallel to the ab-plane. However, it is sufficient for a qualitative investigation, $k = 0.5$ was chosen as the closest fit. The thickness over which supercurrents were allowed to flow was varied between full tape thickness, d, and a quarter of the tape thickness, $0.25d$. The reported results were for superconducting domains with half tape thickness, $0.5d$.

It is worth mentioning what effects the critical state model can account for that the stationary study cannot. Although stationary studies can solve for the FC state of a superconductor with $J_c(B)$, this is only possible for high symmetry cases such as a cylindrical bulk superconductor. The lack of symmetry in our case means that the distribution of current density along the 12 mm width of a single tape piece can be asymmetric about the mid-point. This is because the two sides of the tape pieces can experience different field conditions leading to different J_c. Such asymmetries are not a problem for critical state models. The stationary study used surface current density. This is obviously a good approximation for the HTS layers but it gives rise to a discontinuity in flux lines causing them to bend at a point. This means that the angle of the flux density at the layer is not well defined making J_c anisotropy difficult to implement. Finally, the stationary model cannot simulate time dependent flux creep effects or the magnetization process itself. These reasons motivate more complex critical state modelling in an attempt to better approximate the real experiment.

4.3. Stationary study model results for angled stacks of tape

Figure 7 compares the simple modelling and experimental results for sample A and AB. There was generally good agreement in magnitude for the single stack A. However, for sample AB the experimental data had a lower magnitude than the simple model predicted. The difference can in part be explained by the lack of flux creep in the stationary study model. In both cases the experimental results are clearly more uniform than the model. In section 4.6 the critical state modelling shows some improved agreement with the experimental results.

Figure 8 shows the simulated magnetic field distribution in a single stack, A, and double stack, AB. As mentioned above the tape pieces experience different field conditions, which is particularly apparent at the edges of the sample as can be seen in figure 8(a). This difference could lead to differences in J_c between tapes, particularly as the field angle varies for each piece of tape. Figure 8(b) suggests that the flux lines undergo significant bending within the stacks and that the tape pieces will experience fields at a variety of angles,

Table 2. Descriptions and values of parameters used in critical state modelling.

Parameter	Description	Value
E_0	Electric field constant in equation (2)	1×10^{-4} V m^{-1}
$I_{c0} = I_c$(77 K, SF)	Tape critical current at 77 K and self-field	400 A
w	Tape width	12 mm
d	Tape thickness	100 μm
k	Anisotropy constant in equation (3)	0.5
B_0	Flux density constant in equation (3)	0.192 T
n_0	n-value constant in equation (2)	30
B_{0n}	Flux density constant in equation (2)	0.75 T

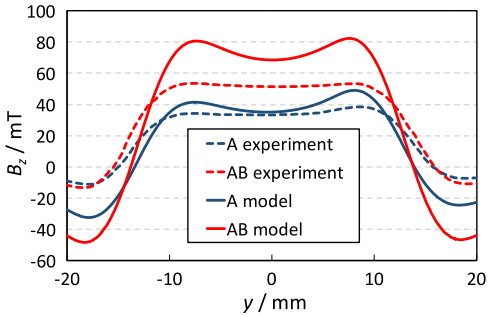

Figure 7. Comparison between modelled and experimental trapped field profiles for samples A and AB.

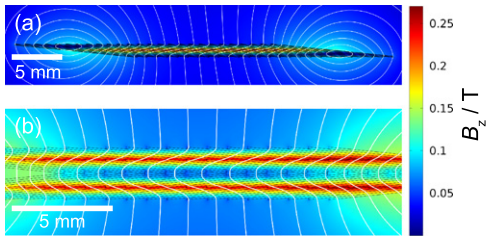

Figure 8. Simulated magnetic field distribution for (a) a single stack, A, and (b) the central region of a double stack, AB. The flux lines show significant bending within the stacks.

not just perpendicular to the superconducting layer. The effect of this $J_c(B, \theta)$ dependence was not incorporated in to the simple stationary study but was investigated as part of the critical state modelling in section 4.6. However, despite the significant flux bending implied in the model the flux decay constant calculated from flux creep measurements, section 3.2, was similar to that for bulks and other stacks of tape.

4.4. Stationary study model results with FM plate

The increase in magnitude and symmetry of the field profiles seen experimentally for samples with the FM plate was reflected in the modelling results shown in figure 9. However, as in the model without the FM plate, the experimental results were more uniform than the model. There was a much better match for the single stack A than the double stack AB. The larger difference for the AB + FM stack could be due to the lack of field dependent J_c, which is more important when the tapes are being exposed to higher field as is the case when

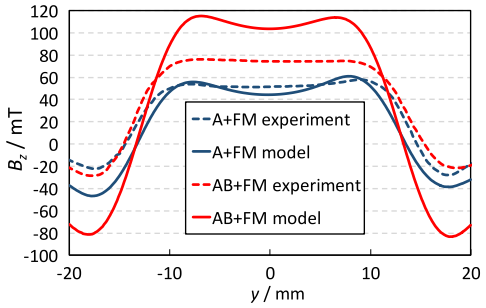

Figure 9. Comparison between modelled and experimental field profiles for samples A+FM and AB+FM.

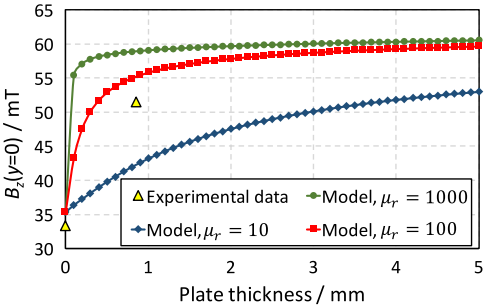

Figure 10. The trapped field magnitude, B_z, with increasing ferromagnetic plate thickness for three different values of relative permeability, μ_r. Experimental data are included for comparison. The measurement height was 2 mm. The plate thickness used in experimental work was 0.85 mm.

adding a FM plate. The FM plate was modelled using a $B(H)$ dependence derived from its measured magnetization curve.

The field enhancement due to the FM plate was expected to increase with increasing plate thickness and permeability [12]. Models with different values of permeability and variable thicknesses of FM plate were solved in the stationary study framework, figure 10. The modelled data all show the FM plate enhancing the field magnitude up to a point where increasing the thickness further does not significantly increase the field magnitude. The results also suggest that the higher the permeability the thinner the plate required to achieve a given increase in trapped field, as expected.

4.5. Stack equivalence to a coil and theoretical best case

The angled stack arrangements give rise to a net current at the sample edges and an approximately zero net current in the

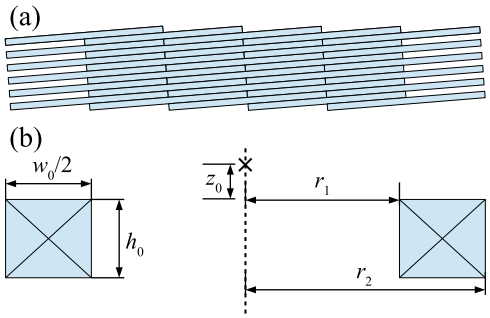

Figure 11. (a) Schematic diagram of the optimum angled stack and (b) the equivalent coil dimensions.

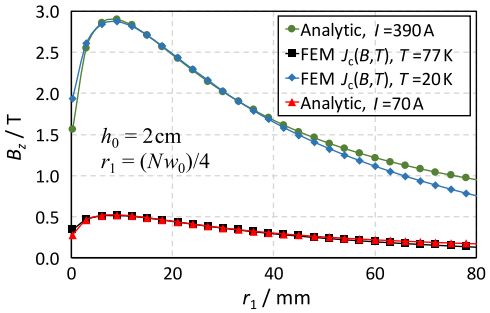

Figure 12. Field 2 mm above coil equivalent for different temperatures and current. Only discrete values of the inner radius, r_1, are allowed due to the way the equivalent stacks can be composed. N = number of tape pieces in a single layer-1.

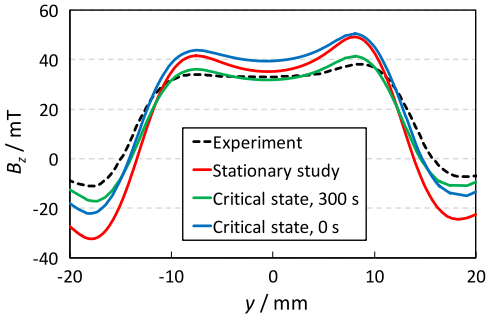

Figure 13. Trapped field profile results for a single angled stack, A. Comparing experimental data with the stationary study and critical state FEM data. The critical state model results 300 s after magnetization showed good agreement with experimental data.

central region. This is explained in detail in appendix B. The simplest angled stack is one where the layers are offset by half their width as shown in figure 11(a). In this case, the only regions contributing net current flow are the half tape width sections at the stack edges. These regions can be approximated by a coil as in figure 11(b) to allow for flexible estimates of the maximum trapped field the angled stacks can produce at different temperatures and sizes. The modelling in this section assumes thin 30 μm tape with 400 A I_c (77 K, SF), which is now commercially available. The previous modelling has considered stacks to be infinitely long hence 2D infinite models. In this case it is more helpful to assume cylindrical symmetry so that the familiar 2D axisymmetric coil equation (B.1) can be used for estimates. Of course, the real experimental stacks have rectangular net currents flowing around the whole sample and so produce a central field somewhere between that resulting from the 2D infinite and 2D axisymmetric approximations.

Although the fields produced by the experimental angled stacks are very uniform, the magnitudes are much lower than the best rare-earth permanent magnets. Lower temperatures and greater stack thickness is needed to reach higher field values. The effect of the coil geometry on the field above the coil is easily calculated from equation (B.1). This was used to estimate the field 2 mm above an ideal stack that had a height of 2 cm. The results are shown in figure 12 for two different critical currents corresponding to 77 and 20 K. For the chosen measurement height of 2 mm, there is an optimum inner radius which gives the highest central field, however larger radii can be used but with reduced field magnitude, as expected for a coil. To calculate the current in the coil at the two different temperatures, the same tape I_c fitting as described in [16] was used to give a field and temperature dependent $J_{c,eng}$. A factor of half is involved due to the 50% space present at the stack edges, figure 11(a). A stationary study model was then used with $J_c(B)$ dependence to calculate the currents and hence field for the coil. Unlike a HTS pancake coil, there was no constraint to make the total current in each tape layer the same. This is because unlike a real coil, the current can be different in each tape layer and hence there is no current constraint for the equivalent coil cross-section. The results of this FEM model are shown in figure 12 and demonstrate large increases in trapped field possible at lower temperatures. The FEM model results are very similar to the analytic coil calculation, which uses uniform current density. The analytic curves were calculated using a current per half tape width that gave an appropriate match in magnitude with the FEM results. The results show that trapped fields above 2.5 T could be expected with a single stack and higher would be predicted between two stacks, thus showing the potential to produce greater fields than possible with rare earth magnets.

4.6. Critical state model results

The trapped field profiles in figure 13 show that the critical state model gave a closer match to experimental data in terms of both magnitude and shape than the stationary study. The time dependent flux creep in the critical state model appears to be a key feature that was not captured by the simpler stationary study and helps to explain the better match with experiment. However, there are still differences between the model and experimental data, most notably in the shape of the profile. As part of the critical state modelling, a sensitivity study was performed to determine if there were parameters that significantly affected the uniformity of the trapped field profile.

The thickness of the superconducting domains was adjusted from 100 μm down to 25 μm to better approximate the thin layer of superconductor in the tape pieces, below this thickness the computation time was too great. No discernible difference was detected in the shape or magnitude of the

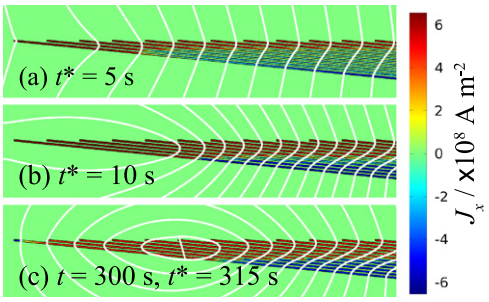

Figure 14. Evolution of current density (a) and (b) during and (c) after the magnetization process. Time $t^* = 0$ is defined as the start of the magnetization ramp, where the external field is reduced. Time $t = 0$ is at the end of magnetization.

trapped field profile when the thickness was altered. The reported model data used a domain thickness of 50 μm. Additionally, the $J_c(B)$ and anisotropic components of the model, k, were adjusted to extreme values to ascertain if they could help explain discrepancy between the model and experimental results. Only small differences in magnitude and negligible differences in shape were noticed. The field and angular dependence of J_c may have only had a very limited effect on the trapped field profiles predicted by the critical state modelling because of the relatively low fields in the angled stacks at 77 K and the expected symmetrical nature of the $J_c(B, \theta)$ curve due to spherical pinning centres. If superconducting tape with more complex $J_c(B, \theta)$ behaviour was used, such as that produced by SuperPower Inc. with columnar defects and vicinal substrate, then the effect of the anisotropic fields experienced by the tape may have a greater effect. Baskys *et al* demonstrated that incorporating experimentally determined angular dependence of J_c in to finite element modelling gave better agreement with experiment for magnetized stacks of tape, particularly at higher fields [19].

The current densities within the tapes during and following magnetization are shown in figure 14. It can be seen that during the ramp down of the applied field the current density is highest at the edge of the tape pieces before reaching a state very similar to that modelled by the stationary study after magnetization. This illustrates that the simple 'block current' used in appendix B and the stack equivalence to a coil are a good approximation.

The critical state modelling results do not fully explain the very high uniformity seen in the experimental trapped fields. There are likely two possible simplifications in the model which may be responsible. The real stacks are not infinitely long in the x direction. The tape pieces at the end of the stack along the y-axis may be experiencing magnetic flux conditions that vary along the x-axis. In other words, there may be complex end effects which would alter the currents in the central tapes and therefore the trapped field profile. The other possibility is that the FEM solution for the tape currents change when the superconducting layer becomes very thin (~microns) giving rise to an altered trapped field. Both these reasons are difficult to investigate numerically due to unmanageable numbers of mesh elements for 3D and thin layer models.

5. Summary

Self-supporting angled stacks of superconducting tape were magnetized and the trapped field profiles above the surface were characterized using Hall probe magnetometry. They were found to produce very uniform trapped field profiles. Multiple layers of the stacks and the addition of a FM plate beneath the samples improved uniformity and magnitude of the trapped fields.

Both stationary and time-dependent critical state finite element modelling in COMSOL multiphysics were performed to complement experimental work. There was found to be good agreement between model and experiment for single stacks in the simple case, which improved further with critical state modelling. Limitations in the simple modelling framework were noticed for multiple layers of the stacks, with the experimental samples displaying lower magnitude but much more uniform field profiles than the model predicted.

The similarities between the magnetized angled stack and a coil were shown and used to predict that the type of stacks investigated have the potential to generate uniform fields much higher than rare-earth magnets. They therefore have the potential to be used in small-scale NMR/MRI devices.

Future work may include trying to magnetize the stacks using pulsed fields, magnetization of the stacks at temperatures lower than 77 K and investigating the magnetic levitation performance of the stacks when used with permanent magnets.

Acknowledgments

The authors would like to thank Dr Massimo Ghidini for assistance with measurement of magnetization curves. Also TBM-W and AB acknowledge the financial support of the Engineering and Physical Sciences Research Council (EPSRC). Data related to this publication are available online at the University of Cambridge data repository: https://www.repository.cam.ac.uk/handle/1810/256002.

Appendix A

To quantify the uniformity of the trapped field profiles a roughness metric, R_{rms}, was used. This quantified the average variation away from the mean trapped field for a set of data. In the current work data were sampled from the central 10 mm of the trapped field profile. The mean trapped field, B^*, is given by (A.1)

$$B^* = \frac{\sum_i^n B_i}{n}, \tag{A.1}$$

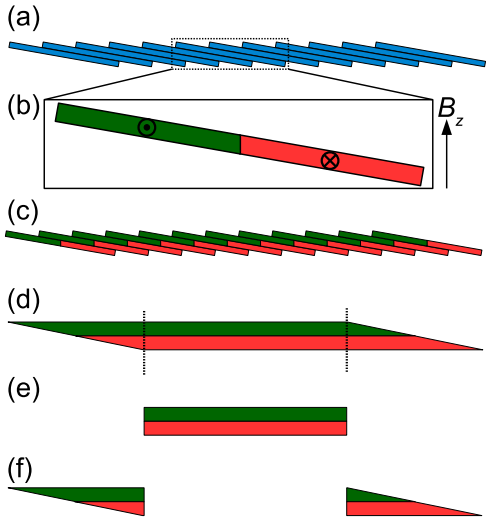

Figure B1. Schematic showing the equivalent block currents in the angled stack A. (a) The single angled stack. (b) A single piece of tape from the stack illustrating the current directions in two domains when magnetized. Block currents rather than surface currents are used for clarity. (c) The block currents in each tape piece are equivalent to a first approximation. (d) Simplification to two domains with opposite current directions, the dotted lines show the boundary between the central and end regions. (e) Central blocks only. (f) End segments only.

where B_i is an individual data point out of n sampled. The roughness is given by (A.2)

$$R_{rms} = \sqrt{\frac{\sum_i^n (B_i - B^*)^2}{n}}. \quad (A.2)$$

Appendix B

The angled stacks were found to have some similarities with a coil when considering the persistent current directions in the magnetized tape layers. This appendix illustrates the equivalence to a coil and includes an equation for the expected field magnitude for a given sample size.

Consider the current directions in a tape piece in a magnetized angled stack as in figure B1(b), the two colours indicating current in opposite directions; the positive and negative x directions. The current in each tape piece can be approximated to a block rather than surface current, which, to a first approximation leads to the schematic in figures B1(b) and (c). This can be further simplified to two current domains as shown in figure B1(d). The relative contribution to the resultant field profile can be deduced by modelling the individual situations shown in figures B1(e) and (f). The results for these models are shown in figure B2. It can be seen that the magnitude of the trapped field measured above the centre is entirely due to the end segments, with the central region only contributing to the shape of the end peaks. Therefore, there is a similarity to a coil with an outer diameter the same as the sample dimensions.

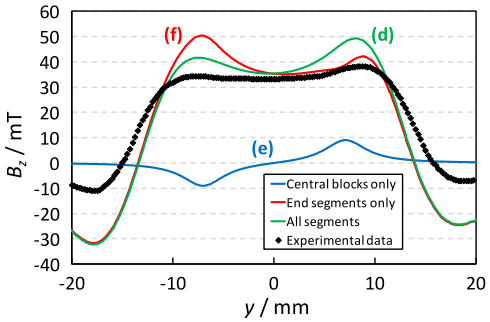

Figure B2. Field profiles from FEM block current models for the separate segments and the complete stack. Experimental data shown for comparison. The modelled profile for block currents in all segments matched exactly with the surface current model used in section 4.3. The central blocks only contribute to the asymmetry of the end peaks; the end segments are responsible for the central field magnitude.

The end segments have an associated engineering current density, $J_{c,eng}$, when considering the net current over their effective area in the y–z plane. To maximize the magnitude of the trapped field the engineering critical current at the edge of the sample needs to be maximized and hence a shallow angled stack was proposed as in section 3.3.

To determine the theoretical limitations of the field achievable with a layered, shallow angled stack an analytic equation was derived for the axial field in a solenoid. The resulting equation (B.1) described how the parameters of inner radius, r_1, outer radius, r_2, tape width, w_0, coil height h_0 and measurement height, z_0, as shown in figure 11(b), all affected the field achievable and matched FEM model results as shown in figure 12

$$B = \frac{\mu_0 \mathrm{In}}{w_0}\left[(z_0 + h_0)\ln\left(\frac{r_2 + \sqrt{{r_2}^2 + (z_0 + h_0)^2}}{r_1 + \sqrt{{r_1}^2 + (z_0 + h_0)^2}}\right) - z_0 \ln\left(\frac{r_2 + \sqrt{{r_2}^2 + {z_0}^2}}{r_1 + \sqrt{{r_1}^2 + {z_0}^2}}\right)\right]. \quad (B.1)$$

References

[1] Tamegai T, Hirai T, Sun Y and Pyon S 2016 Trapping a field of 7.9 T using a bulk magnet fabricated from stacks of coated conductors *Physica* C **0** 1–6
[2] Patel A, Hopkins S C and Glowacki B A 2013 Trapped fields up to 2 T in a 12 mm square stack of commercial superconducting tape using pulsed field magnetization *Supercond. Sci. Technol.* **26** 1–7
[3] Kim S, Nakano T, Takano R and Hahn S Y 2009 Study on trapped field characteristics of HTS bulk annuli with iron rings for ferromagnetic shimming of a compact NMR magnet *IEEE Trans. Appl. Supercond.* **19** 2273–6
[4] Nakamura T, Tamada D, Yanagi Y, Itoh Y, Nemoto T, Utumi H and Kose K 2015 Development of a superconducting bulk magnet for NMR and MRI *J. Magn. Reson.* **259** 68–75

[5] Hahn S, Kim S B, Ahn M C, Voccio J, Bascunan J and Iwasa Y 2010 Trapped field characteristics of stacked YBCO thin plates for compact NMR magnets: spatial field distribution and temporal stability *IEEE Trans. Appl. Supercond.* **20** 1037–40

[6] Hahn S, Kim Y, Voccio J P, Song J, Bascuñán J, Tomita M and Iwasa Y 2014 Temporal enhancement of trapped field in a compact NMR magnet comprising YBCO annuli *IEEE Trans. Appl. Supercond.* **24** 3–7

[7] Selva K and Majkic G 2013 Trapped magnetic field profiles of arrays of (Gd, Y)Ba2Cu3Ox superconductor tape in different stacking configurations *Supercond. Sci. Technol.* **26** 115006

[8] Selva K, Li X-F, Majkic G and Masson P 2015 Assessment of critical factors affecting the performance of trapped field magnets using thin film superconductor tapes *IOP Conf. Ser.: Mater. Sci. Eng.* **102** 012031

[9] Mitchell-Williams T B, Patel A, Baskys A, Hopkins S C, Kario A, Goldacker W and Glowacki B A 2016 Toward uniform trapped field magnets using a stack of roebel cable offcuts *IEEE Trans. Appl. Supercond.* **26** 6800404

[10] Baskys A, Patel A, Hopkins S C, Kalitka V, Molodyk A and Glowacki B A 2015 Self-supporting stacks of commercial superconducting tape trapping fields up to 1.6 T using pulsed field magnetization *IEEE Trans. Appl. Supercond.* **25** 6–9

[11] Samoilenkov S, Molodyk A, Lee S, Petrykin V, Kalitka V, Martynova I, Makarevich A, Markelov A, Moyzykh M and Blednov A 2016 Customised 2G HTS wire for applications *Supercond. Sci. Technol.* **29** 24001

[12] Philippe M P, Ainslie M D, Wéra L, Fagnard J-F, Dennis A R, Shi Y-H, Cardwell D A, Vanderheyden B and Vanderbemden P 2015 Influence of soft ferromagnetic sections on the magnetic flux density profile of a large grain, bulk Y–Ba–Cu–O superconductor *Supercond. Sci. Technol.* **28** 095008

[13] Krabbes G, Fuchs G, Canders W-R, May H and Palka R 2006 *High Temperature Superconductor Bulk Materials* (Weinheim, FRG: Wiley-VCH Verlag GmbH & Co. KGaA) pp 87–8

[14] Selva K, Li X F and Majkic G 2015 Trapped field and flux creep in stacked (Gd,Y)Ba2Cu3Ox superconductor tape arrays *IEEE Trans. Appl. Supercond.* **25** 3–7

[15] Patel A, Baskys A, Hopkins S C, Kalitka V, Molodyk A and Glowacki B A 2015 Pulsed-field magnetization of superconducting tape stacks for motor applications *IEEE Trans. Appl. Supercond.* **25** 1–5

[16] Patel A, Hopkins S, Baskys A, Kalitka V, Molodyk A and Glowacki B A 2015 Magnetic levitation using high temperature superconducting pancake coils as composite bulk cylinders *Supercond. Sci. Technol.* **28** 115007

[17] Chudy M, Zhong Z, Eisterer M and Coombs T 2015 *n* -values of commercial YBCO tapes before and after irradiation by fast neutrons *Supercond. Sci. Technol.* **28** 035008

[18] Zermeno V M R, Abrahamsen A B, Mijatovic N, Jensen B B and Sørensen M P 2013 Calculation of alternating current losses in stacks and coils made of second generation high temperature superconducting tapes for large scale applications *J. Appl. Phys.* **114** 173901

[19] Baskys A, Patel A, Hopkins S C and Glowacki B A 2016 Modeling of trapped fields by stacked (RE)BCO tape using angular transversal field dependence *IEEE Trans. Appl. Supercond.* **26** 6601004